Proceedings of DETC'01
ASME 2001 Design Engineering Technical Conferences and
Information in Engineering Conference
Pittsburgh, Pennsylvania, September 9-12, 2001

DETC2001/VIB-21451

ANALYSIS OF BIFURCATIONS AND CHAOS IN THREE COUPLED PHYSICAL PENDULUMS WITH IMPACTS

Jan Awrejcewicz
Grzegorz Kudra
Technical University of Lodz
Department of Automatics and Biomechanics
1/15 Stefanowskiego St., 90-924 Lodz, Poland
E-mail: awrejcew@ck-sg.p.lodz.pl,
grekudra@ck-sg.p.lodz.pl

C.-H. Lamarque
Ecole Nationale des Travaux Publics de l'Etat /
DGCB / LGM
1 rue Audin, F69 518 Vaulx-en-Velin, France
E-mail: claude.lamarque@entpe.fr

ABSTRACT

In this work the triple pendulum with damping, external forcing and with impacts is investigated. The extension of a coefficient restitution rule and a special transition condition rule for perturbation (linearized system in the Lyapunov exponents algorithm) in each discontinuity point are applied. Periodic, quasi-periodic, chaotic and hyperchaotic motions are observed using Poincaré maps and bifurcational diagrams, which are verified by the Lyapunov exponents. In additon basins of attraction of some coexisting regular and irregular attractors are illustrated and discussed.

1 INTRODUCTION

A pendulum plays a very important role in mechanics since many interesting non-linear dynamical behaviour can be illustrated and analysed using this system (Acheson and Mullin, 1993; Bishop and Clifford, 1996; Skeledon 1994; Yagasaki 1994). Even simple pendulum externally excited can exhibit periodic, quasi-periodic and chaotic dynamics. It is obvious that coupled pendulums with obstacles can serve as a model even for a very complicated behaviour including that of energy pumped to the model, a various amount of resonances, jumps between different system states, various continuous and discontinuous bifurcations, etc.

2 INVESTIGATED PENDULUM AND GOVERNING EQUATIONS WITHOUT IMPACTS

Three joined physical pendulums in the global co-ordinate system x,y,z (with origin in point O_1) are presented in Figure 1.

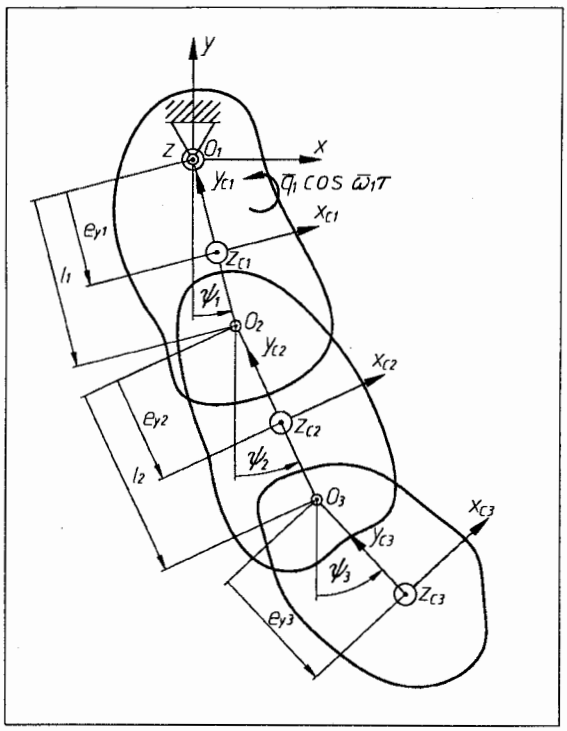

Figure 1. The investigated triple pendulum.

A local co-ordinate system x_{Ci}, y_{Ci}, z_{Ci} formed by principal central co-ordinate axes is attached to each of the i-th link. It is assumed that the links are absolute stiff bodies moving in a vacuum and coupled by viscous damping with the coefficients

$\bar{c}_i$ $(i = 1,2,3)$. The first body is excited by harmonic action $\bar{q}_1 \cos\bar{\omega}_1\tau$, where τ denotes time. In addition it has been assumed, that :

a) the mass centres of the links lie on the lines including the joints O_i;
b) one of the principal central axes of each link (z_{Ci}) is perpendicular to a movement plane of the pendulum ;
c) one of the principal central axes of each link (y_{Ci}) overlaps with a line including the pendulum axes O_i.

The introduced assumptions result in getting symmetric system.

The system position is defined by the angles ψ_i and the folowing generalized-coordinate vector have been chosen

$$\psi = \begin{Bmatrix} \psi_1 \\ \psi_2 \\ \psi_3 \end{Bmatrix}. \tag{1}$$

The governing differential equations of systems without impacts have the following non-dimensional form

$$M \cdot \ddot{\psi} + B \cdot \dot{\psi}^2 + C \cdot \dot{\psi} + D = F, \tag{2}$$

where

$$\ddot{\psi} = \begin{Bmatrix} \ddot{\psi}_1 \\ \ddot{\psi}_2 \\ \ddot{\psi}_3 \end{Bmatrix}, \dot{\psi}^2 = \begin{Bmatrix} \dot{\psi}_1^2 \\ \dot{\psi}_2^2 \\ \dot{\psi}_3^2 \end{Bmatrix}, \dot{\psi} = \begin{Bmatrix} \dot{\psi}_1 \\ \dot{\psi}_2 \\ \dot{\psi}_3 \end{Bmatrix}, \tag{3}$$

M is the 3×3 inertia matrix with the elements

$$\begin{aligned} m_{11} &= 1,\ m_{22} = \beta_2,\ m_{33} = \beta_3, \\ m_{12} &= m_{21} = \nu_{12}\cos(\psi_1 - \psi_2), \\ m_{13} &= m_{31} = \nu_{13}\cos(\psi_1 - \psi_3), \\ m_{23} &= m_{32} = \nu_{23}\cos(\psi_2 - \psi_3), \end{aligned} \tag{4}$$

B is the 3×3 matrix with the elements

$$\begin{aligned} b_{11} &= b_{22} = b_{33} = 0, \\ b_{12} &= -b_{21} = \nu_{12}\sin(\psi_1 - \psi_2), \\ b_{13} &= -b_{31} = \nu_{13}\sin(\psi_1 - \psi_3), \\ b_{23} &= -b_{32} = \nu_{23}\sin(\psi_2 - \psi_3), \end{aligned} \tag{5}$$

C is the 3×3 matrix of damping coefficients

$$C = \begin{bmatrix} c_1 + c_2 & -c_2 & 0 \\ -c_2 & c_2 + c_3 & -c_3 \\ 0 & -c_3 & c_3 \end{bmatrix}, \tag{6}$$

D is the following vector

$$D = \begin{Bmatrix} \sin\psi_1 \\ \sin\psi_2 \\ \sin\psi_3 \end{Bmatrix}, \tag{7}$$

and F is the vector of time-depending external excitations of the form

$$F = \begin{Bmatrix} q_1 \cos(\omega_1 t) \\ 0 \\ 0 \end{Bmatrix}. \tag{8}$$

The relations between dimensional and non-dimensional parameters are as follows

$$\begin{aligned} \beta_2 &= \frac{B_2}{B_1},\ \beta_3 = \frac{B_3}{B_1}, \\ \mu_2 &= \frac{M_2}{M_1},\ \mu_3 = \frac{M_3}{M_1}, \\ \kappa_1 &= \frac{K_1}{B_1},\ \kappa_2 = \frac{K_2}{B_1}, \kappa_3 = \frac{K_3}{B_1}, \\ \nu_{12} &= \frac{N_{12}}{B_1},\ \nu_{13} = \frac{N_{13}}{B_1},\ \nu_{23} = \frac{N_{23}}{B_1}, \end{aligned} \tag{9}$$

$$c_1 = 2\frac{\bar{c}_1}{\sqrt{M_1 B_1}}, c_2 = 2\frac{\bar{c}_2}{\sqrt{M_1 B_1}}, c_3 = 2\frac{\bar{c}_3}{\sqrt{M_1 B_1}}, \tag{10}$$

and

$$q_1 = \frac{\bar{q}_1}{M_1}, \tag{11}$$

where

$$\begin{aligned} B_1 &= J_{z1} + e_{y1}{}^2 m_1 + l_1{}^2(m_1 + m_2), \\ B_2 &= J_{z2} + e_{y2}{}^2 m_2 + l_2{}^2 m_3, \\ B_3 &= J_{z3} + e_{y3}{}^2 m_3, \end{aligned} \tag{12}$$

$$\begin{aligned} M_1 &= m_1 g\ e_{y1} + (m_2 + m_3) g\ l_1, \\ M_2 &= m_2 g\ e_{y2} + m_3 g\ l_2, \\ M_3 &= m_3 g\ e_{y3}, \end{aligned} \tag{13}$$

$$K_1 = J_{x1} - J_{y1} + e_{y1}{}^2 m_1 + l_1{}^2 (m_1 + m_2),$$
$$K_2 = J_{x2} - J_{y2} + e_{y2}{}^2 m_2 + l_2{}^2 m_3, \qquad (14)$$
$$K_3 = J_{x3} - J_{y3} + e_{y3}{}^2 m_3,$$

$$N_{12} = m_2 e_{y2} l_1 + m_3 l_1 l_2,$$
$$N_{13} = m_3 e_{y3} l_1, \qquad (15)$$
$$N_{23} = m_3 e_{y3} l_2.$$

Above J_{xi}, J_{yi}, J_{zi} $(i = 1,2,3)$ denote the appropriate principal inertia momenta and m_i $(i = 1,2,3)$ denote the appropriate masses. The relations between real and non-dimensional time has the form

$$t = \alpha_1 \tau, \qquad (16)$$

where: $\alpha_1{}^2 = \frac{M_1}{B_1}$.

The relations between derivatives with respect to real and non-dimensional time have the forms

$$\frac{d\psi_i}{d\tau} = \alpha_1 \frac{d\psi_i}{dt} = \alpha_1 \dot{\psi}_i, \qquad (17)$$
$$\frac{d^2\psi_i}{d\tau^2} = \alpha_1{}^2 \frac{d^2\psi_i}{dt^2} = \alpha_1{}^2 \ddot{\psi}_i, \qquad i = 1,2,3$$

$$\overline{\omega}_1 = \alpha_1 \omega_1. \qquad (18)$$

Observe that the introduction of the non-dimensional form of the governing equations has decreased the number of parameters (from 23 real parameters to 16 non-dimensional ones). Moreover the non-dimensional equations may govern not only our system of triple pendulum, but also others similar like systems (Bayly and Virgin, 1992; Heng et al. 1994).

3 INTRODUCTION OF THE OBSTACLES TO THE SYSTEM

When in the investigated system the physical rigid obstacles appear, the governing equations can be written as follows:

$$M \cdot \ddot{\psi} + B \cdot \dot{\psi}^2 + C \cdot \dot{\psi} + D = F,$$
$$h_i(\psi) \geq 0, \quad (i = 1,\ldots,n), \qquad (19)$$

where the inequality $h_i(\psi) \geq 0$ represents an unilateral constraint that is imposed on the position of the system, and n is the number of constraints (obstacles).

Since the investigated system (19) is a Lagrangian system, it can be represented as a point moving in its configuration space ψ. Now, it is natural to apply the contact-impacts rules using this representation. More clearly, the unilateral constraints define domains of the configuration space, and the point representing the system strikes the boundaries of these domains. At the times of these „generalized" collisions, one needs to apply additional informations (the restitution rules) in order to calculate the post-impact velocities.

The shock dynamics equations are as follows (Brogliato, 1999):

$$M(\psi) \cdot \sigma_{\dot{\psi}} = p_{\psi}, \qquad (20)$$

where $M(\psi)$ is the inertia matrix (4), p_{ψ} is the generalized percussion vector for coordinates ψ (the force impulse vector due to the impact), and

$$\sigma_{\dot{\psi}} = \begin{Bmatrix} \dot{\psi}_1^+ - \dot{\psi}_1^- \\ \dot{\psi}_2^+ - \dot{\psi}_2^- \\ \dot{\psi}_3^+ - \dot{\psi}_3^- \end{Bmatrix}, \qquad (21)$$

where $\dot{\psi}_i^-$ are the velocities just before impact (due to the time t_k^-) and $\dot{\psi}_i^+$ are the post-impact velocities (due to the time t_k^+), where t_k denotes the impact time.

For frictionless constraints (as we now assume for further consideration) p_{ψ} is defined along $\nabla_{\psi} h_i(\psi)$ (because the interaction force due to the impact takes place along an Euclidean normal to the surface $h_i(\psi) = 0$, which results from the virtual work principle).

Since we know the direction of p_{ψ}, we can obtain three algebraic equations versus four unknowns from equations (21).

In (Brogliato, 1999), the extension of Newton's rule (restitution coeficient rule) to more than one degree-of-freedom systems is considered. It is shown that for a Lagrangian system with generalized coordinates ψ, with a frictionless unilateral constraint $h_i(\psi) \geq 0$, the only possible rule is to apply Newton's restitution rule to the component of $\dot{\psi}$ along $\nabla_{\psi} h_i(\psi)$, which reads:

$$n_{\psi}^T \cdot \dot{\psi}^+ = -e\, n_{\psi}^T \cdot \dot{\psi}^-, \qquad (22)$$

($n_{\psi} = \frac{\nabla_{\psi} h_i(\psi)}{\left\| \nabla_{\psi} h_i(\psi) \right\|}$ is the unitary normal vector, and e is the restitution coefficient), and then to calculate the remaining postimpact velocity components using the shock dynamics equations (20)

$$t_{\psi,1}^T \cdot M(\psi) \cdot \begin{Bmatrix} \dot{\psi}_1^+ - \dot{\psi}_1^- \\ \dot{\psi}_2^+ - \dot{\psi}_2^- \\ \dot{\psi}_3^+ - \dot{\psi}_3^- \end{Bmatrix} = 0,$$

$$t_{\psi,2}^T \cdot M(\psi) \cdot \begin{Bmatrix} \dot{\psi}_1^+ - \dot{\psi}_1^- \\ \dot{\psi}_2^+ - \dot{\psi}_2^- \\ \dot{\psi}_3^+ - \dot{\psi}_3^- \end{Bmatrix} = 0, \qquad (23)$$

where $t_{\psi,1}$ and $t_{\psi,2}$ are the tangent unitary vectors chosen as mutually independent, i.e. $t_{\psi,1}^T \cdot \nabla_\psi h_i(\psi) = 0$, $t_{\psi,2}^T \cdot \nabla_\psi h_i(\psi) = 0$ and $t_{\psi,1}^T \cdot t_{\psi,2} = 0$.

Any other rule is just a consequence of that, plus Newton's law of an action-reaction.

It can be also shown, that for a restitution coefficient $e = 1$, the kinetic energy change due to the impact is equal to zero.

From the equations (23) one realizes that in general there exist a discontinuity in the tangential velocity due to inertia coupling.

4 CALCULATION OF THE LYAPUNOV EXPONENTS

The fourth order Runge-Kutta method with detection of each point of an impact with an arbitrary precision has been used to integrate the obtained system of ordinary differential equations. In each impact point the system state has been transformed using equations (22) and (23).

The Lyapunov exponents have been computated directly from the differential equations using well known algorithm (Wolf et al., 1985). Because of discontinuities, a linearized system which represents the motion perturbation have been transformed (Müller, 1995) in each point of a discontiniuty using special rules.

Let x denotes the state vector of the system, i.e.:

$$x^T = [\psi_1, \dot{\psi}_1, \psi_2, \dot{\psi}_2, \psi_3, \dot{\psi}_3, \omega_1 t], \qquad (24)$$

then the equations (2) can be written in the following form

$$\dot{x} = f(x(t)). \qquad (25)$$

The time evaluation of the tangent vector $\delta x(t)$ at $x(t)$ is represented by the linearized equation (25)

$$\dot{\delta x} = F(t)\delta x(t), \qquad (26)$$

where:

$$F(t) = \left.\frac{\partial f(x)}{\partial x^T}\right|_{x=x(t)}. \qquad (27)$$

The spectrum of the Lyapunov exponents λ_i ($i = 1,..,7$ for our 7-dimensional dynamical system) is given for seven different linearly independent initial conditions $\delta x_i(t_0)$

$$\lambda_i = \lim_{t\to\infty} \frac{1}{t} \ln \frac{\|\delta x_i(t)\|}{\|\delta x_i(t_0)\|}. \qquad (28)$$

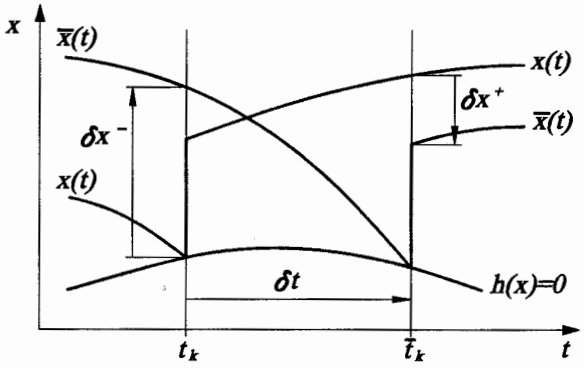

Figure 2. Undisturbed and disturbed motion.

When the nonlinear system at $t = t_k$ reaches the discontinuity point (see Figure 2) indicated by $h(x(t_k^-)) = 0$, then the state vector $x(t)$ is transformed by the relation

$$x(t_k^+) = g(x(t_k^-)), \qquad (29)$$

where $g(x)$ in our case is given by (22) and (23).
The disturbed motion $\bar{x}(t)$ is defined by

$$\bar{x}(t) = x(t) + \delta x(t), \qquad (30)$$

and it encouters a discontinuity at the time $\bar{t}_k$

$$\bar{t}_k = t_k + \delta t. \qquad (31)$$

The transition condition for perturbation $\delta x(t)$ is given in (Müller, 1995) and has the following form

$$\begin{aligned} \delta x^+ &= G(x(t_k^-))\delta x^- + \\ &+ [G(x(t_k^-))f(x(t_k^-)) - f(x(t_k^+))]\delta t, \end{aligned} \qquad (32)$$

where:

$$\delta t = -\frac{H(x(t_k^-))\delta x^-}{H(x(t_k^-))f(x(t_k^-))}, \qquad (33)$$

$$H(x)=\frac{\partial h(x)}{\partial x^T}, \tag{34}$$

$$G(x)=\frac{\partial g(x)}{\partial x^T}. \tag{35}$$

5 NUMERICAL EXAMPLES

A special simple case of the introduced system of coupled physical pendulums will be further analysed. We consider only three identical rods with damping, external excitation q_1 and with the obstacle in the form of horizontal wall (Figure 3).

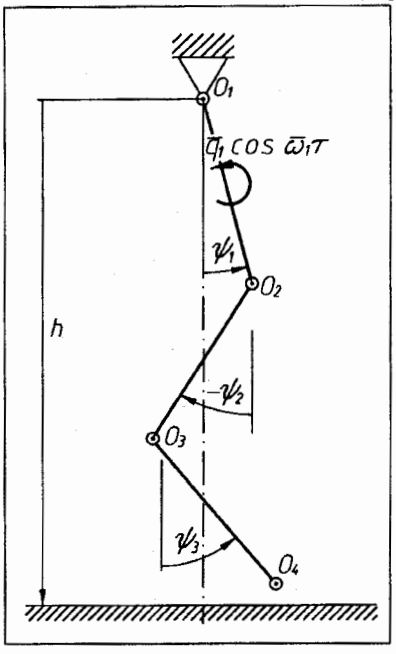

Figure 3. Three coupled rods with the obstacle.

The physical obstacle can be expressed in the following non-dimensional form

$$\begin{aligned} h_1(\psi)&=\eta-\cos\psi_1\geq 0,\\ h_2(\psi)&=\eta-(\cos\psi_1+\lambda_2\cos\psi_2)\geq 0,\\ h_3(\psi)&=\eta-(\cos\psi_1+\lambda_2\cos\psi_2+\lambda_3\cos\psi_3)\geq 0, \end{aligned} \tag{36}$$

where:

$$\lambda_2=\frac{l_2}{l_1},\quad \lambda_3=\frac{l_3}{l_1},\quad \eta=\frac{h}{l_1}, \tag{37}$$

and l_i is the real length of the i-th rod and h is the real position of the horizontal wall.

For three identical rods we have

$$\lambda_2=1,\quad \lambda_3=1, \tag{38}$$

and others non-dimensional parameters read

$$\begin{aligned} &\beta_2=\frac{4}{7},\quad \beta_3=\frac{1}{7},\\ &\mu_2=\frac{3}{5},\quad \mu_3=\frac{1}{5},\\ &\kappa_1=1,\quad \kappa_2=\frac{4}{7},\quad \kappa_3=\frac{1}{7},\\ &\nu_{12}=\frac{9}{14},\quad \nu_{13}=\frac{3}{14},\quad \nu_{23}=\frac{3}{14}. \end{aligned} \tag{39}$$

We present (see Figures 4-7) some numerically obtained examples for three identical coupled rods with the physical obstacle introduced in Figure 3.

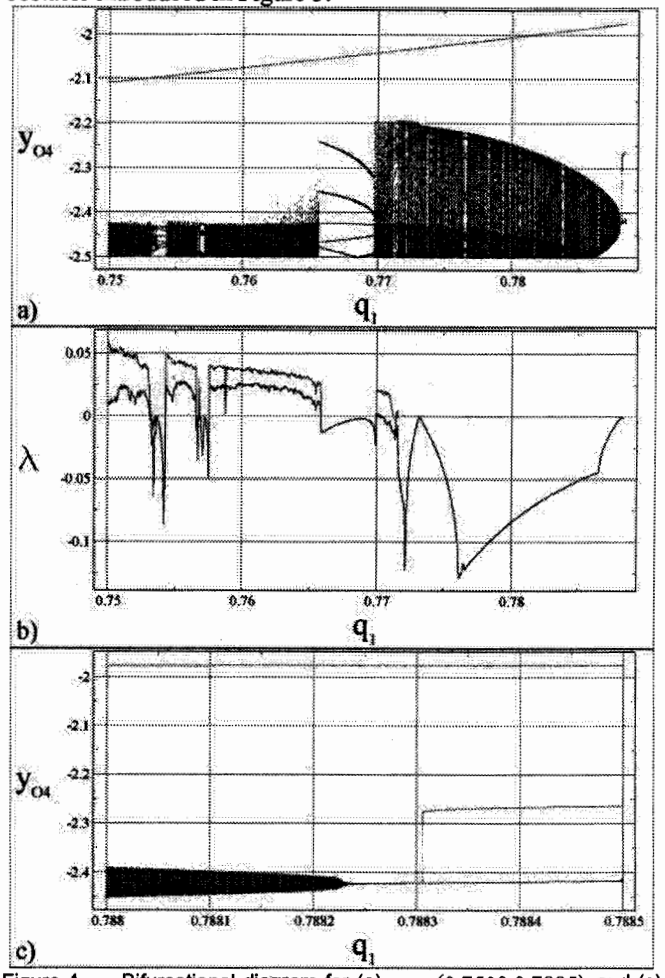

Figure 4. Bifurcational diagram for (a) $q_1 \in (0.7500,0.7885)$ and (c) $q_1 \in (0.7880,0.7885)$; three coexisting solutions (blue, green and red), where y_{O4} denotes the third rod's end co-ordinate; and the coresponding two largest Lyapunov exponents (b) (except of zero exponent) corresponding to 'blue' solution.

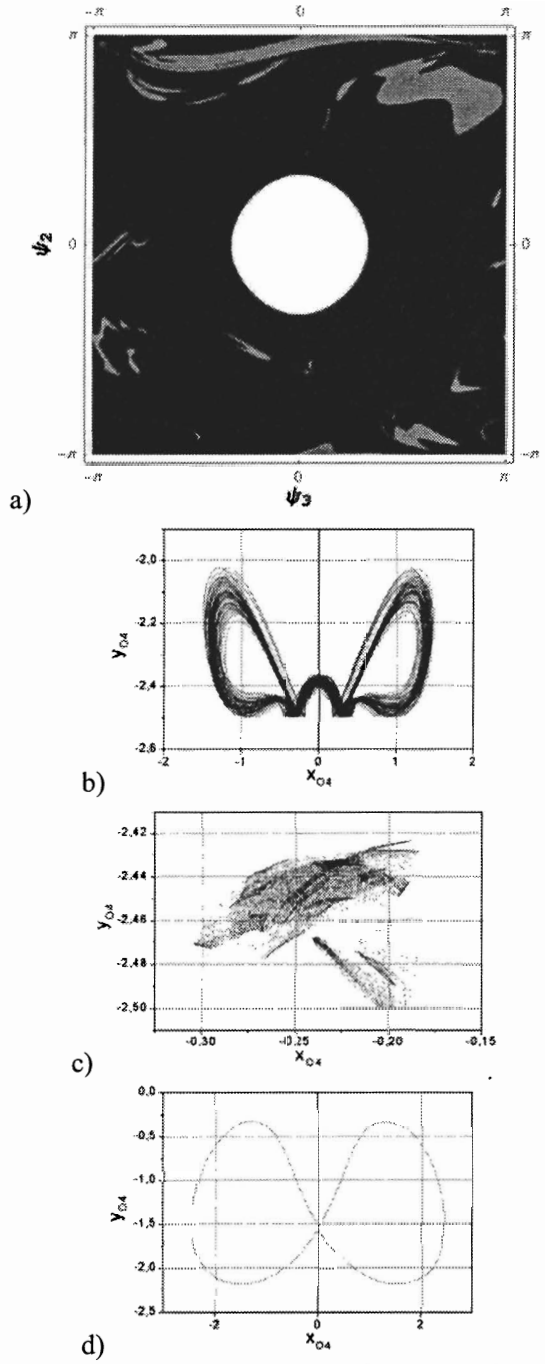

Figure 5. Basins of attraction (a) of two coexisting solutions (corresponding to $q_1 = 0.75$ in Figure 4) with the initial conditions: $\psi_1(t=0)=0$, $\psi_2(0)\in(-\pi,\pi)$, $\psi_3(0)\in(-\pi,\pi)$, $\dot{\psi}_1(0)=\dot{\psi}_2(0)=\dot{\psi}_3(0)=0$; phase trajectories (b,d) and Poincaré map (c); blue – hyperchaotic solution, green – periodic one for $t\in(2000,2500)$ (b); $t\in\left(2\cdot10^3,10^5\right)$ - 15597 points (c); $t\in(100,125)$ (d).

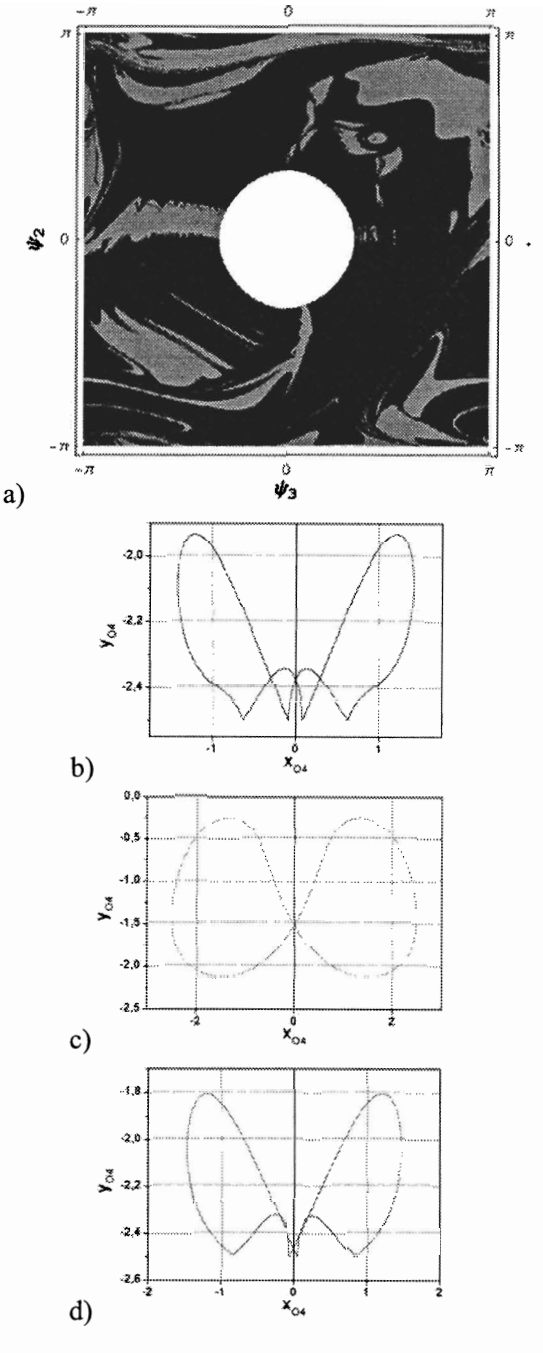

Figure 6. Basins of attraction (a) for three coexisting periodic solutions (corresponding to $q_1 = 0.7885$ in Figure 4); initial conditions the same as in Figure 5; phase trajectories (b,c,d) for $t\in(5000,5050)$ (b); $t\in(100,125)$ - 15597 points (c); $t\in(5000,5050)$ (d).

The following parameters are fixed: $\eta = 2.5$, $e=1$, $c_1 = c_2 = c_3 = 0.1$ and $\omega_1 = 1$. The q_1 parameter has been varied within the interval $(0.75, 0.7885)$ and the initial conditions of the system are varied, too. In the considered

interval three different solutions have been detected, and their biffurcational histories are reported in Figure 4. The first one (green) is always beeing periodic one and our pendulum motion takes place without any impact. The pendulum omits the obstacle (see Figure 5d and Figure 6c). The second solution (red) is also periodic but with impacts (see Figure 6d), and it vanishes for $q_1 = 0.788106$ (see Figure 4c). The third periodic solution (blue) is of most importance, since it undergoes a route to hyperchaos when q_1 is decreased. For instance for $q_1 = 0.7885$ it is periodic, whereas for $q_1 = 0.788232$ it bifurcates to quasi-periodic solution (see Figure 4c). The quasi-periodic solution for $q_1 = 0.786$ and its discontinuous Poincaré section are shown in Figure 7.

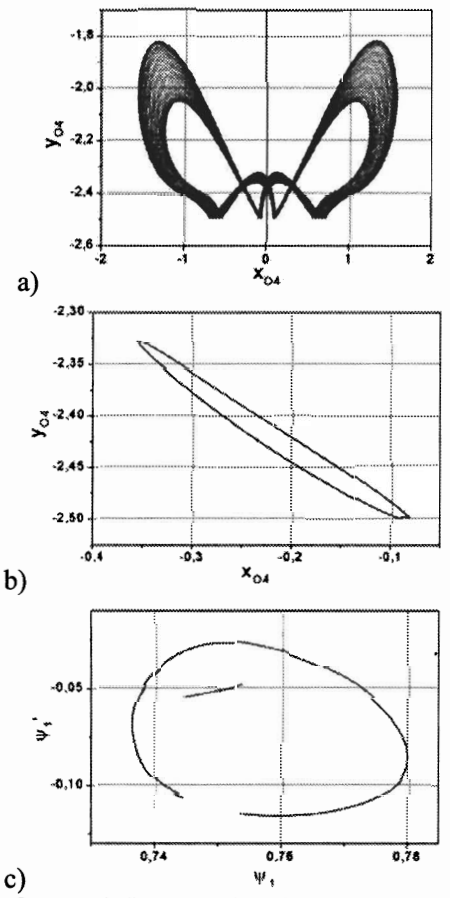

Figure 7. Quasi-periodic solution (a – phase trajectory) corresponding to $q_1 = 0.786$ (see Figure 4) with the discountinuous Poincaré section (b,c) for $t \in (5000,5050)$(a); $t \in (5 \cdot 10^3, 2 \cdot 10^4)$ (b,c).

A further decrease of q_1 causes a transition to chaos for $q_1 = 0.7715$ with a short periodic window. For $q_1 = 0.7700$ again a relatively large periodic orbit domain occurs, which dissapears for $q_1 = 0.7659$. Then the hyperchaos occurs, which is observed until the end of the considered interval of q_1. The hyperchaos is interrupted by narrow periodic windows for $q_1 \in (0.7530, 0.7543)$ and $q_1 \in (0.7566, 0.7576)$, which with a high probability include also quasi-periodic and chaotic intervals. However, the latter ones are difficult distinguishable in Figure 6c.

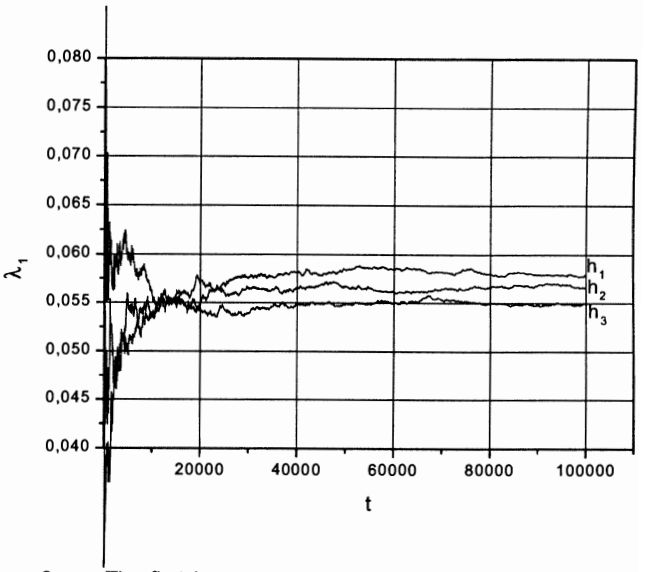

Figure 8. The first Lyapunov exponent for the solution shown in Figure 5 b/c (hyperchaotic motion) for three different integral time steps: $h_1 = 2\pi/1000$, $h_2 = 2\pi/400$ and $h_3 = 2\pi/200$.

The corresponding Lyapunov exponents are shown in Table 1. The largest Lyapunov exponent corresponding to hyperchaos for different integration steps has been reported in Figure 8.

Figure	5 b/c	5 d	6 b	6 c	6 d	7 a/b/c
λ_1	0.06	0	0	0	0	0
λ_2	0.01	-0.010	-0.0017	-0.11	-0.14	0.0000
λ_3	0	-0.010	-0.0017	-0.11	-0.28	-0.0469
λ_4	-0.67	-0.25	-0.0660	-0.26	-0.28	-0.0470
λ_5	-0.94	-0.25	-1.2626	-0.26	-0.28	-1.2963
λ_6	-1.48	-1.69	-1.7733	-1.71	-1.39	-1.6679
λ_7	-2.10	-2.40	-1.7733	-2.29	-2.56	-1.8376

Table 1. The lyapunov exponents λ_i $(i = 1,\ldots,7)$ for the analysed solutions.

6 CONCLUDING REMARKS

In this report we have analysed regular and irregular dynamics of triple pendulum with damping, external excitations and impacts and with physical obstacle in the form of horizontal wall. The impact law for triple pendulum in the form of generalized Newton's rule has been introduced, and other special transition conditions for disturbed motion in each impact point have been applied.

Periodic, quasi-periodic and hyperchaotic motions have been detected, discussed and illustrated. The basins of attraction

for three coexisting periodic solutions have been reported, and a transition to hyperchaos has been illustrated.

REFERENCES

Acheson, D. J. and Mullin, T. "Upside down pendulums," *Nature* **366**, 215-216, 1993.

Bishop, S.R. and Clifford, M.J. "Zones of chaotic behavior in the parametrically excited pendulum," *J. Sound Vib.* **189**(1), 142-147, 1996.

Brogliato, B. *Nonsmooth Mechanics.* Springer-Verlag, London, 1999.

Bayly, P. V. and Virgin, L. N. "Experimental evidence of diffusive dynamics and random walking in a single deterministic mechanical system: the shaken pendulum," *Int. J. Bifurcation and Chaos* **2**(4), 983-988, 1992.

Heng, H. Doerner, R. Hübinger, B. and Marfienssen, W. "Approaching nonlinear dynamics by studying the motion of a pendulum, I: observing trajectories in state space," *Int. J. Bifurcation and Chaos* **4**(4), 751-760, 1994.

Müller, P. "Calculation of Lyapunov exponents for dynamic systems with discontinuities." *Chaos, Solitons and Fractals* **5**(9), 1971-1681, 1995.

Skeledon, A. C. "Dynamics of a parametrically excited double pendulum," *Physica* **D75**, 541-558, 1994.

Yagasaki, K. "Chaos in a pendulum with feedback control," *Nonlin. Dyn.* **6**, 125-142, 1994.

Wolf, A. & Swift, B. & Swinney, H. & Vastano, J. "Determining Lyapunov exponents from a time series," *Physica* **D16**, 285-317, 1985.